

## Simultaneous In-situ Analysis of Instabilities and First Normal Stress Difference during Polymer Melt Extrusion Flows

Roland Kádár<sup>1,2</sup>, Ingo F. C. Naue<sup>2</sup> and Manfred Wilhelm<sup>2</sup>

<sup>1</sup> Chalmers University of Technology, 41258 Gothenburg, Sweden

<sup>2</sup> Karlsruhe Institute of Technology - KIT, 76128 Karlsruhe, Germany

### ABSTRACT

A high sensitivity system for capillary rheometry capable of simultaneously detecting the onset and propagation of instabilities and the first normal stress difference during polymer melt extrusion flows is here presented. The main goals of the study are to analyse the nonlinear dynamics of extrusion instabilities and to determine the first normal stress difference in the presence of an induced streamline curvature via the so-called hole effect. An overview of the system, general analysis principles, preliminary results and overall framework are herein discussed.

### INTRODUCTION

Capillary rheometry is the preferred rheological characterisation method for pressure-driven processing applications, e.g. extrusion, injection moulding. Capillary rheometry is the only method of probing material rheological properties in processing-like conditions, i.e. high shear rate, nonlinear viscoelastic regime, albeit in a controlled environment and using a comparatively small amount of material.<sup>1</sup> Thus, it is of paramount importance to develop new techniques to enhance the capillary rheometers for a more comprehensive probing of material properties. Extrusion alone accounts for the processing of approximately 35% of the worldwide production of plastics, currently  $280 \times 106$  tons (Plastics Europe, 2014). This makes it the most important single polymer processing operation for the industry and can

be found in a variety of forms in many manufacturing operations. Extrusion throughput is limited by the onset of instabilities, i.e. product defects. Comprehensive reviews on the subject of polymer melt extrusion instabilities can be found elsewhere.<sup>4,6</sup> A recent method proposed for the detection and analysis of these instabilities was that of a high sensitivity in-situ mechanical pressure instability detection system for capillary rheometry.<sup>8,10</sup> The system consists of high sensitivity piezoelectric transducers placed along the extrusion slit die. In this way all instability types detectable thus opening new means of scientific inquiry. As a result, new insights into the nonlinear dynamics of the flow has been provided.<sup>9,14</sup> Moreover, the possibility of investigating the reconstructed nonlinear dynamics was considered, whereby a reconstructed phase space is an embedding of the original phase space.<sup>2,14</sup> It was shown that a positive Lyapunov exponent was detected for the primary and secondary instabilities in linear and linear low density polyethylenes, LDPE and LLDPE.<sup>14</sup> Moreover, it was determined that Lyapunov exponents are sensitive to the changes in flow regime and behave qualitatively different for the identified transition sequences.<sup>14</sup> It was also shown that it is possible to transfer the high sensitivity instability detection system to lab-sized extruders for inline advanced processing control and quality control systems.<sup>13</sup>

A very recent possibility considered

concerns the use of the high sensitivity instability detection system for the measurement of the normal stress differences via the hole effect. Errors in pressure measurements for polymeric liquids, i.e. with non-zero normal components of the extra-stress tensor, we known for decades to occur for offset positioned transducer with respect to the capillary walls.<sup>5</sup> This effect was used by Lodge for the determination of the first normal stress difference, i.e. the Lodge stressmeter.<sup>5</sup> However, many challenges still remain for the implementation and to achieve a desired accuracy for such methods.<sup>7,12</sup>

## EXPERIMENTAL

The experimental setup is based on a Göttert Rheotester 2000 capillary rheometer featuring a custom slit die. The die is equipped with four high sensitivity piezoelectric pressure transducers, Fig. 1.a, and has an aspect ratio of  $W/H = 10$ , where  $W$  and  $H$  are the channel width and height respectively ( $W = 3\text{ mm}$ ,  $H = 0.3\text{ mm}$ ). The transducers are capable of delivering remarkable time and pressure resolutions, namely  $10^{-3}\text{ s}$  and  $10^{-5}\text{ bar}$  at a nominal pressure of 500 bar. Three of the transducers, Tr1-Tr3, are equally spaced along the channel length, whereas the fourth, Tr4, is facing Tr3 with flush or offset positioning with respect to the flow channel. The Tr4 offset can be accordingly adjusted to induced streamline curvature and thus create the so called 'hole effect' for the estimation of the normal stress difference(s), Fig. 1.b. Complementary, an online visualisation system is positioned at the die exit for advanced image analysis.

The experimental protocols for the testing consist of quasi ramped input signals, similarly to a typical protocol for capillary rheometry measurements. In contrast, the stabilisation times for each shear rates were imposed via scripting in order to bypass all take-over procedures. Two experimental protocols were applied to cover from

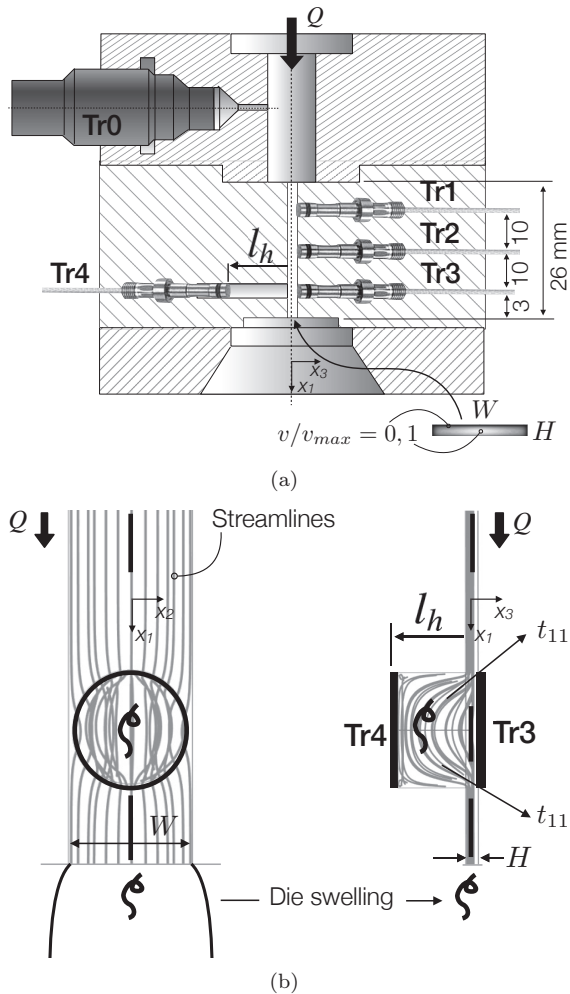


Figure 1. (a) Schematic representation of the high sensitivity extrusion die and the corresponding transducer placement, Tr1,2,3. Tr0 represents a conventional pressure transducer. (b) Detailed positioning of the facing Tr3,4 transducers used to induced streamline curvature.

low to high apparent shear rates. A constant quasi-linear ramp rate of  $d\dot{\gamma}_a/dt = 0.76 \times 10^{-3}\text{ s}^{-2}$  was applied in the former case, with  $\dot{\gamma}_a = 6Q/WH^2$  being the apparent shear rate, whereas in the latter case a nonlinear protocol was used. Other parameters varied are the hole depth, see  $l_h$  in Fig. 1, operating bulk temperature and draw ratio. The latter was imposed using a Rheotens device however here only zero draw ratios are presented.

Commercial samples with different molecular characteristics, i.e. linear / short chain branched and branched topologies were considered. In this publication two samples are emphasised, a low density polyethylene (LDPE) having  $T_m = 111^\circ\text{C}$ ,  $M_w = 186\text{ kg/kmol}$  and  $M_w/M_n = 12$  and a high density polyethylene (HDPE) having  $T_m = 131^\circ\text{C}$  (data provided by the manufacturers).

The oscillatory shear measurements presented were performed on a TA Instruments ARES-G2 rheometer.

## RESULTS AND DISCUSSION

An example of typical mechanical pressure output from the in-situ transducers is presented in Fig. 2. The diagram features the raw mechanical pressure signals as well. Piezoelectric transducers are mainly dedicated to fast transient processes, therefore, additional data treatment was necessary for the present experiments. Thus, a steady state load can be expressed using the condition  $dp_M/dt = s$ , where  $s$  is the drift. Using the conventional mechanical pressure data, Tr0 in Fig. 1.a, a drift correction was considered,  $dp_M/dt = 0$ , whereby

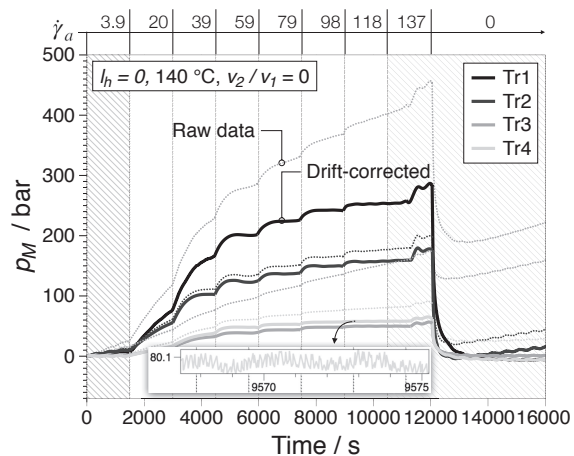


Figure 2. Example of output signal showing the raw and the drift corrected signals for all transducers. Data for an

LDPE having  $T_m = 110^\circ\text{C}$ ,  $M_w = 256\text{ kg/kmol}$  and  $M_w/M_n = 15$ , tested at  $140^\circ\text{C}$  with  $l_h = 0$ .

a linear function of slope  $s$  is subtracted from the raw data, i.e. drift corrected data. More details on data pre-processing are provided elsewhere.<sup>9,14</sup> Overall, the signals in Fig. 2 contain two contributions, namely a nominal value of the mechanical pressure, based on which the hole pressure is determined, and the fluctuations superimposed on the signal, based on which the onset of instabilities can be in-situ detected. It should be noted that the data displayed in the figure already exhibits an inherent pressure difference between Tr3 and Tr4, although the Tr4 was in flush positioning,  $l_h = 0$ . This residual difference was subtracted from subsequent hole pressure measurements for the determination of the first normal stress difference.

The time dependent mechanical pressure data showing the influence of hole depth,  $l_h = H, 6H, 20H$ , is presented in Fig. 3.a for both low and high apparent shear rate experimental protocols. The onset of instabilities is marked on the diagrams whenever available from the analysis of the in-situ mechanical pressure fluctuations and spatio-temporal inline visualisations. Spatio-temporal visualisations, or space-time plots, are constructed by extracting a line of pixels out of a collection of frames and then successively add them to a new visualisation, a common method in fluid dynamics.<sup>11,14</sup> An example of the latter is presented in Fig. 3.b. With respect to the nominal pressure, it can be seen and increase in the pressure difference between Tr3 and Tr4 is increased between  $l_h = H$  and  $l_h = 6H$ . However, for  $l_h = 20H$  the mechanical pressure decreases, which could indicate the occurrence of secondary flows. By comparing the low and high shear rate tests there it is apparent that there is no significant influence of the dynamical history, i.e. the quasi-linear ramp rate, in the steady-state mechanical pressure. The stationarity of the flow for each apparent shear rate step can be analysed with respect to the existence of mechanical pres-

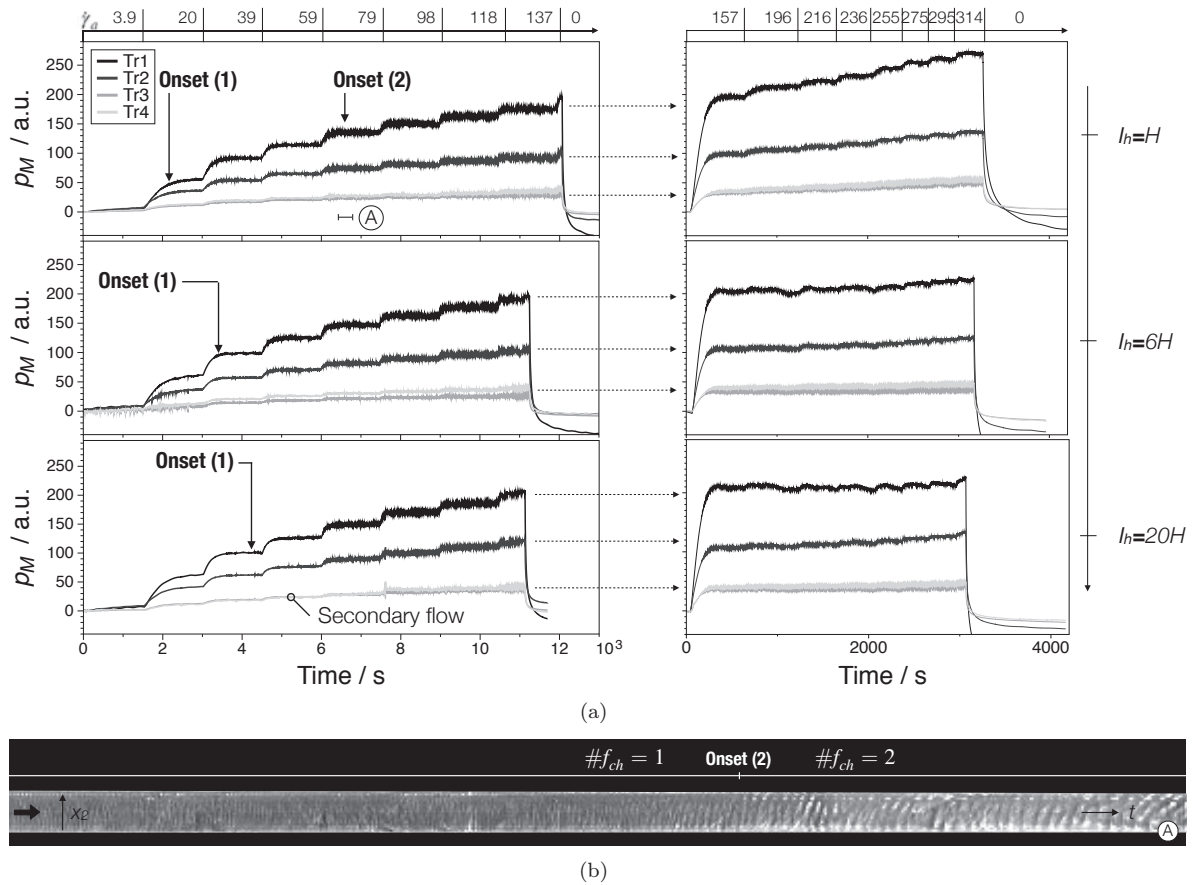


Figure 3. (a) Influence of of hole depth,  $l_h$  on the time dependent in-situ mechanical pressure for the two inout protocols used in the study, i.e. for the low shear rate and high shear rate range. (b) Spatio-temporal visualisation, corresponding to region A in (a), showing the transition from the primary to the secondary instability type. Data for an LDPE having  $T_m = 111$  °C,  $M_w = 186$  kg/kmol and  $M_w/M_n = 12$  , tested at 180 °C.

sure fluctuations associated to the instabilities observed in LDPE using recurrence plots. Such an example is presented in Fig. 4 and corresponds to the  $\dot{\gamma} = 79 \text{ s}^{-1}$  step of the  $l_h = H$  test in Fig. 3.a. A recurrence plot comprises of mechanical pressure points  $p_{M_i}, p_{M_j}$  who have an interdistance smaller than  $\Delta p_m / 10^3$  in a embedded vector. The embedding is performed in the framework of Takens' embedding theorem.<sup>2</sup> The depicted recurrence plot considers embedding dimensions equal to 2 and 3, with the delay time being determined based on previous results.<sup>14</sup> For an unsteady flow the points are correlated on the diagonal whereas for steady-state flows they spread over the adjacent domain.

Examples of transient Fourier transform (FT) analysis of Tr1,2,3,4 are shown in Fig. 5, corresponding to the  $l_h = H$  mechanical pressure date in Fig. 3.a for the low shear rate test. Overall, there are two main contributions to the FT spectra for supercritical extrusion flows: (i) the characteristic pattern frequencies, i.e. the surface and/or volume extrudate distortions observed and (ii) a low frequency contribution to the spectra.<sup>14</sup> Other miscellaneous identified contributions include the electrical network frequency (50 Hz for the EU) and the machine engine, e.g. see Fig. 6. It can thus be seen that while the low frequency contributions to the spectra are identifiable in all transducers it is difficult

to identify peaks that could be associated to the inline optical observations of extrudate patterns.

In order to identify the pattern contributions a different approach can be applied. Thus, it is assumed that the pattern frequency contributions are detected only using the transducers positioned close to the die exit.<sup>14</sup> Therefore, the spectra of Tr1 can be subtracted from the Tr3,4, with an appropriate scaling coefficient. Furthermore, to compensate for the shortcoming of using a linear scaling, a circular colour map can be used. An example of such differential transient FT diagrams is presented in Fig. 6 for the low and high shear rate test,  $l_h = H$ . The onset of extrudate pattern characteristic frequencies and the supercritical bifurcation behaviour can thus be observed. In the case of a branched structure, i.e. LDPE, the nonlinear dynamics feature the onset of a first instability type having one characteristic (extrudate pattern) frequency,  $f_{ch1}$ .<sup>14</sup> With increasing shear rate a lower frequency component is

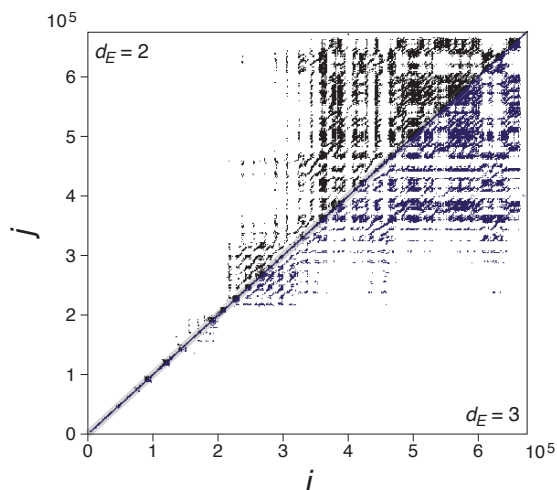


Figure 4. Recurrence plot of the LDPE data in Fig. 3.a,  $l_h = H$ ,  $\dot{\gamma} = 79 \text{ s}^{-1}$  showing the onset of stationarity, where  $i, j$  represent the indexes of points having a distance smaller than  $\Delta p_m / 10^3$  in a 2-dimensional and 3-dimensional reconstructed phase space.

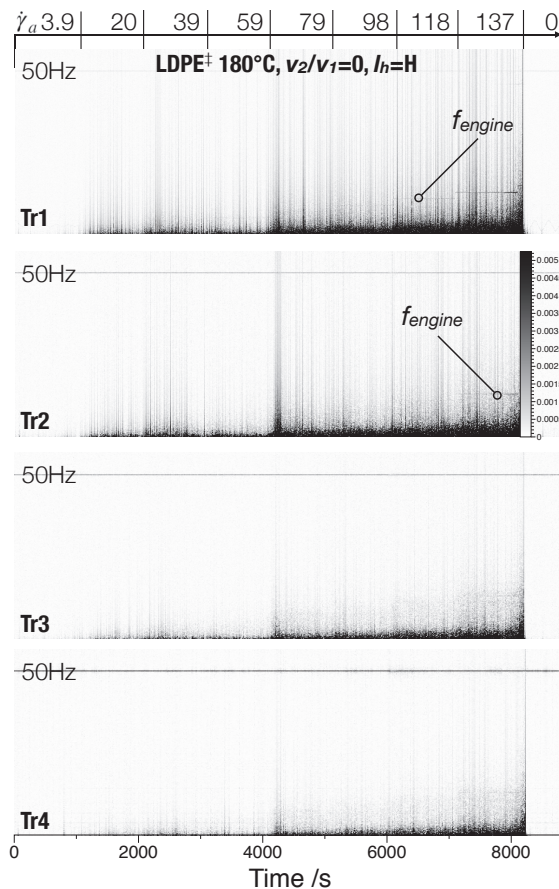


Figure 5. Transient Fourier transform analysis of the in-situ mechanical pressure fluctuations. The data corresponds to the diagrams in Fig. 3.

superimposed on the base one, and the resulting pattern is identified as having two characteristic frequencies,<sup>14</sup>  $f_{ch1}$  and  $f_{ch2}$ , e.g. see also Fig. 3.b. At the highest shear rates higher harmonics of the fundamental are also readily distinguishable. Overall, the increasing hole depth has a stabilising effect on the flow, i.e. the onset of instabilities is postponed. Moreover, the onset of the second instability type was not identifiable in the spectra for  $l_h > H$ . Finally, it is important to note that the signal corresponding to the onset and propagation of instabilities is read in both Tr3 and Tr4 transducers regardless of the hole depth.

For contrast, similar data is briefly presented for the HDPE sample mentioned. For such short chained branched/linear

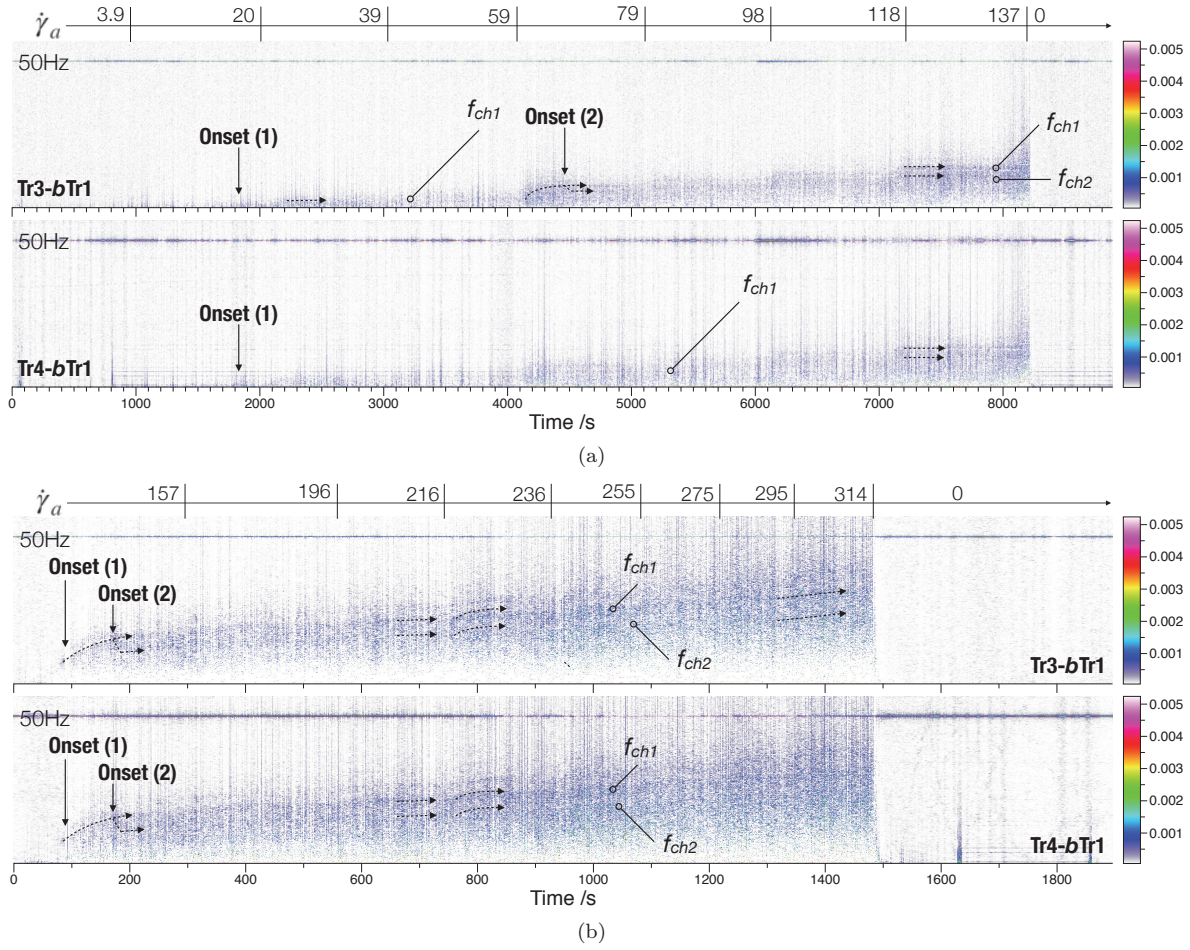


Figure 6. Differential transient Fourier transform analysis of showing the onset of instabilities and supercritical bifurcations for the data in Fig. 3.a,  $l_h = H$  in the data of Tr3,4, using (a) low and (b) high shear rate experimental protocols.

molecular architectures, smooth extrudate flow is replaced with increasing apparent share rate with the sharkskin instability, having one characteristic pattern frequency. The secondary instability type detected is that of stick-slip for which three characteristic frequencies are identifiable in the spectra.<sup>14</sup> An example of such a transition sequence is presented in Fig. 7 as spatio-temporal visualisation. The visualisation corresponds to region B in Fig. 9. The influence of hole depth on the nominal value of the mechanical pressure for the HDPE sample is shown for the low, Fig. 8, and high, Fig. 7, apparent shear rate test ( $l_h = H$ ). It can be observed that the increasing hole depth has a destabilising ef-

fect on the flow, i.e. the stick-slip regime is triggered at lower shear rates. The effect on the onset of the sharkskin instability was no conclusive from the tests. In addition, a strong influence on the history of deformation is observed between the low and high apparent shear rate tests in the case of HDPE. The normal stress difference can be computed from the curved streamline tests based on the hole pressure  $\Delta p_h = a_1 N_1 + a_2 N_2$  where  $\Delta p_h = p_{Tr3} - p_{Tr4}$  is the hole pressure,  $N_1 = t_{11} - t_{22}$ ,  $N_2 = t_{22} - t_{33}$  the first and second normal stress difference and  $a_1$ ,  $a_2$  the corresponding proportionality coefficients. For a circular opening with neglectable  $N_2$  the first normal stress difference can be determined as<sup>5</sup>

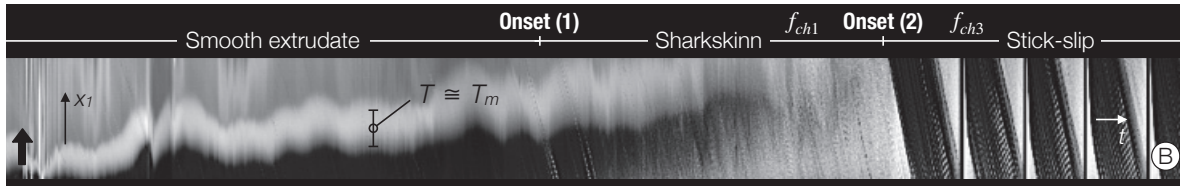


Figure 7. Spatio-temporal visualisation corresponding to the region B in Fig. 9 showing the transition from smooth extrudate to the primary instability, i.e. sharkskin, and further to the secondary instability type, i.e. stick-slip.

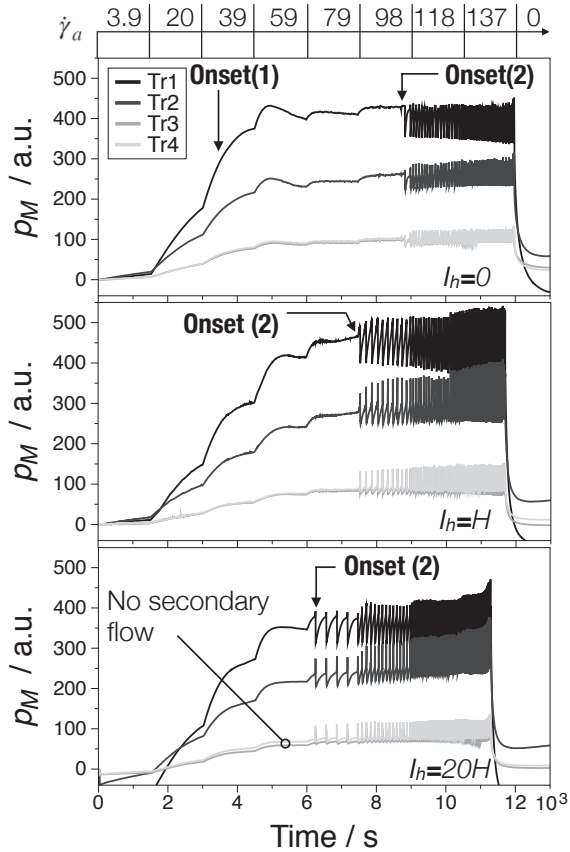


Figure 8. Influence of hole depth,  $l_h$  on the time dependent in-situ mechanical pressure for the low apparent shear rate region HDPE having  $T_m = 131^\circ\text{C}$ , tested at  $180^\circ\text{C}$ .

$N_1 \approx 0.25 \cdot \Delta p_M$  ( $a_1 = 4$ ,  $a_2 = 0$ ). For validation, such data is compared with oscillatory shear measurement via the the Laun rule:<sup>3</sup>

$$N_1^{\text{Laun}}(\dot{\gamma}) = 2G'(\omega) \left( 1 + \left( \frac{G'(\omega)}{G''(\omega)} \right)^2 \right)^{0.7} \quad (1)$$

where  $G'$  and  $G''$  are the dynamic moduli

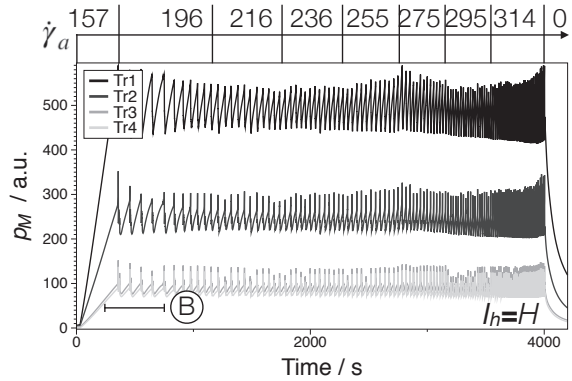


Figure 9. High shear rate mechanical pressure time dependence for an HDPE having  $T_m = 131^\circ\text{C}$ , tested at  $180^\circ\text{C}$ .

determined from oscillatory tests. Such a comparison is presented in Fig. 10 for the LDPE sample. It can be seen that a good agreement is found for the  $a_1 = 4$  case and  $l_h = 6H$ . It could thus be asserted that for  $l_h = H$  the hole pressure recorded is not sufficient for accurate readings whereas for  $l_h = 20H$  secondary flows may be responsible for altering the measurements.

## SUMMARY AND CONCLUSIONS

A high sensitivity piezoelectric system for capillary rheometry capable of simultaneous in-situ detection and analysis of instabilities and determination of the first normal stress difference during polymer melt extrusion flows was briefly described in this publication. The transition sequences detected in the presence of curved streamlines were presented. The analysis of the in-situ hole pressure shows that with careful data processing procedures it is possible to determine (at least) the first normal

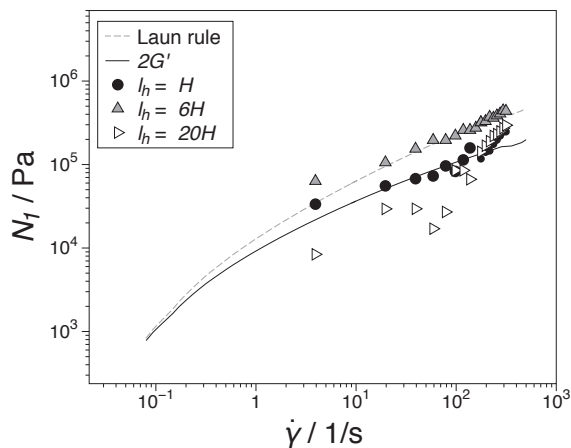


Figure 10. Comparison between the first normal stress determined through capillary rheometry with results obtained from oscillatory shear tests via the Laun rule the the LDPE sample at 180 °C.

stress difference using the high sensitivity system.

#### ACKNOWLEDGEMENTS

The study was financed by the German Science Foundation, DFG grant WI 1911/14-1. The authors are grateful to Dr. I. Vittorias of LyondellBasell and Dr. S. Filipe of Borealis for providing the test samples.

#### REFERENCES

1. Walters, K. (1975), "Rheometry", Chapman and Hall, London.
2. Takens, F. (1981), "Detecting strange attractors in turbulence", in "Lecture Notes in Mathematics, Dynamical Systems and Turbulence", Rand, D. and Young, L.-S.
3. Laun, H. M. (1986), "Prediction of Elastic Strains of Polymer Melts in Shear and Elongation", *Journal of Rheology*, **30**, 459-501.
4. Larson, R. (1992), "Instabilities in viscoelastic flows", *Rheol. Acta*, **31**, 213-263.
5. Barnes, H. A., Hutton, J. F. and Walters, K. (1998), "An introduction to rheology", Elsevier, Amsterdam [u.a.].
6. Denn, M. (2001), "Extrusion Insta-

bilities And Wall Slip", *Ann. Rev. Fluid Mech.*, **33**, 265-287.

7. Baird, D. (2008), "First normal stress difference measurements for polymer melts at high shear rates in a slit-die using hole and exit pressure data", *J. Non-Newtonian Fluid Mech.*, **148**, 13-23.

8. Palza, H., Naue, I. F. C. and Wilhelm, M. (2009), "In situ Pressure Fluctuations of Polymer Melt Flow Instabilities: Experimental Evidence about their Origin and Dynamics", *Macromol. Rapid Commun.*, **30**, 1799-1804.

9. Palza, H., Filipe, S., Naue, I. and Wilhelm, M. (2010), "Correlation between polyethylene topology and melt flow instabilities by determining in-situ pressure fluctuations and applying advanced data analysis", *Polymer*, **51**, 522-534.

10. Palza, H., Naue, I., Filipe, S., Becker, A., Sunder, J., Göttfert, A. and Wilhelm, M. (2010), "On-line Detection of Polymer Melt Flow Instabilities in a Capillary Rheometer", *Kautsch. Gummi Kunstst.*, **63**, 456-461.

11. Kádár, R. and Balan, C. (2012), "Transient dynamics of the wavy regime in Taylor-Couette geometry", *Eur. J. Mech. B. Fluids*, **31**, 158 - 167.

12. Teixeira, P. F., Hilliou, L., Covas, J. A. and Maia, J. M. (2013), "Assessing the practical utility of the hole-pressure method for the in-line rheological characterization of polymer melts", *Rheol. Acta*, **52**, 661-672.

13. Ratzsch, K.-F., Kádár, R., Naue, I. F. C. and Wilhelm, M. (2013), "A Combined NMR Relaxometry and Surface Instability Detection System for Polymer Melt Extrusion", *Macromol. Mater. Eng.*, **298**, 1124-1132.

14. Kádár, R., Grosso, M., Naue, I. F. and Wilhelm, M. (2014), "Reconstructed dynamics of in situ mechanical pressure fluctuations during the extrusion flow of polyethylene melts", (Manuscript in preparation).